ARTICLE

BIOTECHNOLOGY and BIOENGINEERING

Micro-Raman Spectroscopy of Algae: Composition Analysis and Fluorescence Background Behavior

Y.Y. Huang,[1] C.M. Beal,[2] W.W. Cai,[2] R.S. Ruoff,[2] E.M. Terentjev[1]

[1]Cavendish Laboratory, University of Cambridge, Cambridge, UK

[2]Department of Mechanical Engineering, Cockrell School of Engineering, University of Texas at Austin and the Texas Materials Institute, 1 University Station C2200, Austin, Texas 78712; telephone: 512-471-4691; fax: 512-471-7681; e-mail: r.ruoff@mail.utexas.edu

Received 5 June 2009; revision received 30 September 2009; accepted 20 November 2009

Published online ? ? ? ? in Wiley InterScience (www.interscience.wiley.com). DOI 10.1002/bit.22617

ABSTRACT: Preliminary feasibility studies were performed using Stokes Raman scattering for compositional analysis of algae. Two algal species, *Chlorella sorokiniana* (UTEX #1230) and *Neochloris oleoabundans* (UTEX #1185), were chosen for this study. Both species were considered to be candidates for biofuel production. Raman signals due to storage lipid (specifically triglycerides) were clearly identified in the nitrogen-starved *C. sorokiniana* and *N. oleoabundans*, but not in their healthy counterparts. On the other hand, signals resulting from the carotenoids were found to be present in all of the samples. Composition mapping was conducted in which Raman spectra are acquired from a dense sequence of locations over a small region of interest. The spectra obtained for the mapping images were filtered for the wavelengths of characteristic peaks that correspond to components of interests (i.e., triglyceride or carotenoid). The locations of the components of interest could be identified by the high intensity areas in the composition maps. Finally, the time-evolution of fluorescence background was observed while acquiring Raman signals from the algae. The time dependence of fluorescence background is characterized by a general power law decay interrupted by sudden high intensity fluorescence events. The decreasing trend is likely a result of photo-bleaching of cell pigments due to prolonged intense laser exposure, while the sudden high intensity fluorescence events are not understood.

Biotechnol. Bioeng. 2009;9999: 1–10.

KEYWORDS: algae; Raman; triglyceride; lipid; composition analysis; biodiesel

Introduction

To date, analysis of algae composition is a multi-staged process. At the beginning, each cell component is isolated by centrifugation and solubilization. These purified extracts are subsequently analyzed by techniques such as mass spectroscopy and high-pressure liquid chromatography (HPLC) to determine their chemical formula and their relative abundance (Gillan and Johns, 1983; Guschina and Harwood, 2006; Nischwitz and Pergantis, 2006; Schmid and Stich, 1995). These procedures can be slow, tedious and require a substantial amount of algae. Due to the growing emphasis on the large-scale production of algae for fuels and chemicals, a fast composition analysis technique is needed. Rapid composition analysis, potentially using Stokes Raman scattering, would greatly facilitate the selection of suitable algal strains and their associated growing conditions for different applications, ranging from biofuels to nutritional supplements (Demirbas, 2007; Radmer and Parker, 1994; Sheehan et al., 1998; Thompson, 1996).

Raman scattering has traditionally been used as a vibrational spectroscopy technique complementary to infrared spectroscopy for composition analysis. It has a key advantage when applied to biological samples due to its low sensitivity to water content (Frank and Parker, 1983a). In normal conditions, the Raman scattering intensity of an active component depends on the incident laser frequency to the fourth power (Smith and Dent, 2005). The intensity of a characteristic peak also scales linearly with the concentration of the molecule which produces the spectrum. However, resonant scattering (Chao et al., 1975) occurs when a molecule's absorption maxima are close to the incident laser frequency (or excitation energy). Resonant scattering has great resolution, down to 10^{-8} M, compared to the 10^{-3} M resolution limit of conventional Raman scattering. Coherent anti-Stokes Raman scattering, CARS, (Begley et al., 1974) is a technique based on the resonant scattering phenomenon described above and has been used in the areas of lipid quantification, lipid metabolism investigation, and the associated label free imaging technique (Xie et al., 2006). For general biological samples, Stokes Raman scattering (Frank

Correspondence to: R.S. Ruoff

and Parker, 1983b) is less suitable than CARS since the Stokes effect requires much higher excitation laser power than CARS to produce reasonable signals (Xie et al., 2006), leading to potential photo-damage of the samples. Nevertheless, Stokes Raman scattering is more wide-spread and technologically simpler than CARS; therefore, Stokes Raman scattering has a better opportunity for fast industrial implementation.

Our prime aim was to conduct a feasibility study on proof-of-principal, using simple, conventional Stokes Raman scattering effects to analyze the composition of algae, with specific emphasis on identifying the presence of storage lipid, that is, triglyceride (Guschina and Harwood, 2006; Thompson, 1996). This motivation is stemmed from the increasing interest in algal biofuel production. The first part of this manuscript is dedicated to composition analysis of *Chlorella sorokiniana* (UTEX #1230) and *Neochloris oleoabundans* (UTEX #1185), comparing our results and data with the reference absorption spectra in the literature. The composition analysis was conducted by acquiring Raman spectra from the algal samples and identifying key component peaks, and then Raman image scans were employed to map the composition of a single cell or many cells. Secondly, an investigation into the change in fluorescence background during long time laser exposure was carried out, through which some unexpected dynamics of algal cells' response to high laser intensity were noted, characterized by high intensity fluorescence events that are not fully understood.

Materials and Methods

Algae Treatment and Sample Preparation

C. sorokiniana (UTEX #1230) and *N. oleoabundans* (UTEX #1185) were obtained from the UTEX algae culture collection at the University of Texas at Austin. Several different samples were used in this study and the growth conditions varied slightly for each specimen. Generally speaking, healthy samples (grown in Bold 3N media) and nitrogen-starved samples (grown in modified Bold 3N media containing no nitrogen) of both *C. sorokiniana* and *N. oleoabundans* were obtained (contents of Bold 3N media include H_2O, $NaNO_3$, $CaCl_2{\cdot}2H_2O$, $MgSO_4{\cdot}7H_2O$, K_2HPO_4, NaCl, and Vitamin B_{12}. cf. UTEX, www.utex.org). The nitrogen starvation was applied in order to enhance the lipid production in cells and the term "starved" refers to nitrogen starvation throughout the remainder of this document. Information regarding the growth media and starvation period is listed in Table I for each of the samples used in this study. The starvation was conducted by inoculating a fresh batch of modified Bold 3N media that lacked nitrogen (i.e., lacking $NaNO_3$) with a healthy sample, thus beginning the starvation period. All of the liquid cultures were grown at UTEX with continuous aeration (1.5% CO_2 in air), no agitation, 15 W/m^2 of continuous lighting (using F32/T8 fluorescent bulbs), and at a room temperature of about 70°F for their entire growth, except for *Starved NeoO #2* which was subjected to additional starvation as detailed in Table I. The agar culture was also grown at UTEX on agar slants.

To prepare a liquid specimen for confocal micro-Raman spectroscopy, an algal culture was concentrated by centrifugation, after which glass microscope slides coated with poly-L-lysine were placed in the solution in a Petri dish. After a few hours, the slides (with algae adhered) were taken out and the excess water on the glass surface was removed by gently blowing compressed difluoroethane across the sample. The samples were taken for analysis immediately after slide preparation. For our purpose of determining triglyceride content in cells, an in vivo experimental condition is not essential. The agar culture required even less preparation, in which a small volume of the agar and algae material was placed on a microscope slide and spread out slightly.

Confocal Raman Spectroscopy and Microscopy

Raman spectra were measured by a WITec Alpha 300 Confocal Raman Microscope with a 532 nm excitation wavelength. All measurements were performed at room temperature, and the saturation intensity level for data acquisition was $\sim 6 \times 10^4$ counts. The maximum output laser power was estimated to be ~5 mW over a focused spot of ~0.5 μm diameter, giving a power density of ~25 kW/mm^2 over the focal depth of ~1 μm. We chose to work with such a high power density because preliminary tests indicated that the majority of the characteristic peaks could only be revealed after increased laser power. While it is

Table I. Sample Growth Conditions

	Sample name	Species	Growth medium	Starvation duration
1	*Healthy ChloS*	*Chlorella sorokiniana*	Bold 3N	NA
2	*Starved ChloS*	*Chlorella sorokiniana*	Bold 3N w/o nitrogen	7–14 days
3	*Healthy NeoO*	*Neochloris oleoabundans*	Bold 3N	NA
4	*Starved NeoO*	*Neochloris oleoabundans*	Bold 3N w/o nitrogen	7–14 days
6	*Healthy NeoO Agar*	*Neochloris oleoabundans*	Agar slant	NA
7	*Starved NeoO #2*	*Neochloris oleoabundans*	Bold 3N w/o nitrogen	~53 days[a]

[a]Grown in nitrogen deficient media in continuous lighting and aeration for 7 days and then sealed, removed from aeration, and subjected to 12 h of light per day for 46 days at room temperature (~72°F).

possible that cell functions were damaged by irradiation, our main purpose was to identify the triglyceride content. We note that optical microscopy examination (50×) indicated that the cells remained intact (although likely dehydrated) and the Raman spectra indicated that they were not burned after illumination for ~5 min.

As mentioned, when the laser excitation energy is close to one of the electronic transitions of the molecule under investigation, resonant Raman scattering will occur (Spiro, 1974). Therefore, our first task was to evaluate the electronic transitions of the different constituent molecules in algae with respect to the excitation wavelength (532 nm). DNA/RNA, proteins, fats (including triglyceride), polysaccharide, and various pigments (e.g., chlorophylls and carotenoids) are the major chemical constituents of algal cells. By studying the UV/Vis-NIR absorption spectra of these cell components, it was found that except for the photosynthetic pigments, most cell components (including lipids) in plants do not absorb in the visible range (~400–700 nm). On the other hand, one finds general broad absorption bands in the ~400–520 and 650–700 nm regions for different green and brown algae (Yang et al., 1991), which are mostly due to chlorophylls (absorption peaks at ~400–480 and 650–700 nm; Oba et al., 1997) and carotenoids (500–550 nm; Gaier et al., 1991). With the 532 nm excitation wavelength used in our experiments, resonant scattering is therefore expected only for carotenoids.

Data Collection and Processing

Chemical composition analysis of algae was carried out through collecting Raman spectrum from individual cells of healthy and nitrogen-starved *C. sorokiniana* and *N. oleoabundans*. For the composition identification, each spectrum is an average of 10 accumulations, each with an integration time of 0.2 s, and acquired at the same location within the cell. Therefore, these spectra were acquired in a few seconds. With a confocal setup, spectral information is only collected from the laser focal region (in our case ~0.20 μm^3), which is inhomogeneous. In order to identify the mean cell composition, a number of points were chosen within each cell to acquire Raman spectra. These spectra were baseline corrected using a Rolling-Circle-Filter (RCF) (see below), and then normalized against the 0 cm^{-1} intensity before taking an average. Spectra were recorded within the wavenumber region of −300 and 3,200 cm^{-1} at a spectral resolution of 2.4 cm^{-1}.

Most spectra collected contained a pronounced background, which is likely caused by fluorescence of the pigments in algal cells. Since the spectral backgrounds do not contain any chemical-specific information, they were usually omitted in previous studies by baseline correction using different mathematical procedures, for example, Heraud et al. (2006). To separate the fluorescence background, the raw spectra obtained were subjected to a RCF, a high-pass filter that can provide efficient background subtraction without introducing significant distortion to the high frequency components (Brandt et al., 2006). During the RCF process, the original spectrum was split into two parts of information to be analyzed; the characteristic peaks associated with the local cell composition, and the fluorescence background level induced by laser exposure (cf. Fig. 1, plot a). Throughout the data processing, no data smoothing was applied. To interpret the results, the mean spectra were compared to the literature reports of various algae and common biological molecules (Brahma et al., 1983; Heraud et al., 2006, 2007; Kubo et al., 2000; Largeau et al., 1980; Wood et al., 2005). The reference graphical data were extracted using *Engauge Digitizer*, and then interpolated to the same wavenumber points as those used in our tests by linear interpolation (interp1, Matlab).

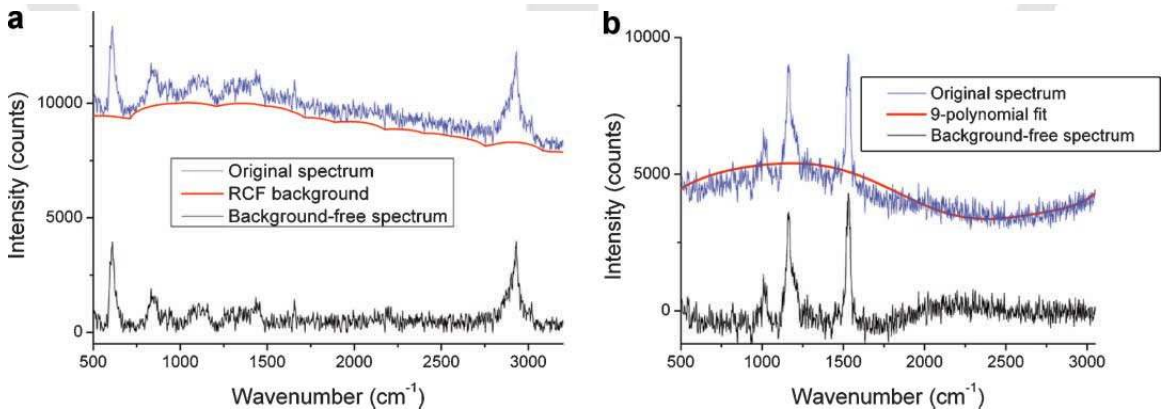

Figure 1. **a**: A raw spectrum from a starved *N. oleoabundans* (*Starved NeoO*) sample illustrating the RCF baseline correction method applied to the spectra used for chemical identification. The original spectrum (blue line) is split into the characteristic peaks associated with the local cell composition (black line) and the fluorescence background (red line). **b**: A raw spectrum from the healthy *N. oleoabundans* agar sample (*Healthy NeoO Agar*) (blue line) is shown alongside with the 9th order polynomial fit used to determine the background level of Raman mapping (red line). The resulting spectrum after the polynomial background subtraction is also shown (black line).

Chemical composition mapping was also performed to identify and locate carotenoids in healthy *N. oleoabundans* cells and triglyceride in starved *N. oleoabundans* cells. For the mapping images, spectra were acquired at a dense sequence of locations within the algal cells and the relative peak intensities were compared to identify and locate compounds of interest. The spectra from every location, that is, each pixel, were background subtracted and then filtered for a wavenumber region that corresponds to a signature peak in the spectrum of either carotenoid or triglyceride. Based on the relative intensity within the specified wavenumber band, the pixels were then colored according to a gradient that ranges from black (low intensity) to red (medium intensity) to yellow (high intensity), thus identifying and locating the components. The spectra that compose the Raman maps were acquired with the same spectral range and resolution as those for composition identification. The chemical composition maps required roughly 1 h of acquisition time, depending on the spatial resolution and spectral integration time specified (cf. Chemical Composition Mapping Section).

To reduce computation time, a 9th order polynomial background subtraction (included in the WITec software) was applied for the chemical mapping spectra rather than using the RCF background subtraction. Figure 1, plot b displays an example of the polynomial baseline subtraction. This method is able to preserve the characteristic peaks, despite yielding an uneven reference level, and is adequate for the purpose of mapping a characteristic peak. (Although not used in this study, a segmented polynomial curve fit could be used to reduce the influence of the peaks on the background.) As with all spectroscopy methods, interference can obscure the results. For the components of interest in this study, β-carotene and triglyceride, we have reasonably high confidence that the characteristic peaks are distinct enough (as compared to common biological molecules present in algae (de Gelder[Q2], 2007; Hendra and Agbenyega, 1993) to discern the location of those particular compounds. The potential interference is discussed in more detail below.

As mentioned previously, independent information about the fluorescence background level can also be extracted following the RCF process. The sum of the background counts over the 0–3,200 cm^{-1} spectral range provides a quantitative indicator to the level of fluorescence "emitted" during a particular time interval for data acquisition. Dynamics of Raman Signal Evolution Section investigates the change of this indicator with respect to the length of laser exposure, reflecting some interesting phenomena which may be explained by the cells' dynamic response to high-light intensity.

Results

Chemical Identification

The Raman spectrum of an entire cell is formed by the spectra convolution of a large number of biological molecules. The relative contribution of each component depends on its relative abundance and the corresponding detection sensitivity (i.e., incident laser wavelength). Knowledge of the Raman spectrum for generic triglyceride is required in order to "visualize" the storage lipids in algae. These molecules consist of a glycerol backbone and three long chain fatty acid tails. Triglyceride composition depends on the constituent fatty acids, which can vary in chain length (n), degree of saturation, or position(s) of the double bond(s) (Bresson et al., 2005; Hu et al., 2008). Raman spectra are largely unaffected by the chain length (n) of a fatty acid when $n > 11$. Any presence of unsaturated carbon bonds in the methylene chain will induce additional peaks at ~1,265 cm^{-1} (δ(=CH)), ~1,650 cm^{-1} (ν(C=C)), and 3,000 cm^{-1} (ν(=CH)) compared to a saturated chain. However, the position of carbon–carbon double bonds, when they are present, does not alter the spectrum to a large extent (Bresson et al., 2005). For the triglycerides present in green micro-algae, of which fatty acid chains are predominantly long chain unsaturated (Guschina and Harwood, 2006), we expect the Raman spectra to be largely similar. This implies that Raman scattering may not distinguish the exact type of triglyceride produced in an alga. This can be seen as an advantage because one does not need to carry out extensive sampling of various triglycerides, and the analysis of triglyceride content in algae is then reduced to "spotting" and "fitting" only a single spectral pattern. Also, it is likely that biodiesel can be produced from all types of triglyceride produced by algae, and thus it is not critical to distinguish between different types. Previous studies have produced biodiesel from algal lipids that has similar properties to those required by ASTM biodiesel standards (Li et al., 2007; Miao and Wu, 2006) (for ASTM standards, cf. Durret et al., 2008; Knothe, 2006). Based on the above information, glyceryl trioleate (Sigma[Q3] T7140) was selected as a representative for generic unsaturated triglyceride. Figure 2 shows the Raman spectrum of glyceryl trioleate obtained under the same conditions as those of algae.

The next stage is to examine whether triglyceride has distinct bands compared to other bio-molecules. A comprehensive database on the Raman spectra of various key biological molecules has been provided by de Gelder et al. (2007). They report that the triglyceride spectra exhibit distinctly different Raman patterns from other abundant molecules in cells such as, DNA, RNA, and amino acids. This difference is expected because the overall structures of the biological molecules listed above are very different. Although two of the intense bands for triglyceride exist in the wavenumber region of ~1,000–1,450 cm^{-1}, and thus overlap with those arising from some saccharide types, triglyceride can be distinguished by the characteristic peak at ~1,650 cm^{-1} or the broad peak between ~2,800 and 3,000 cm^{-1}. Further support for using the broad wavenumber band to identify lipids is provided by several previous studies conducted with CARS that have used peak locations of ~2,840 or 2,845 cm^{-1} to identify lipids

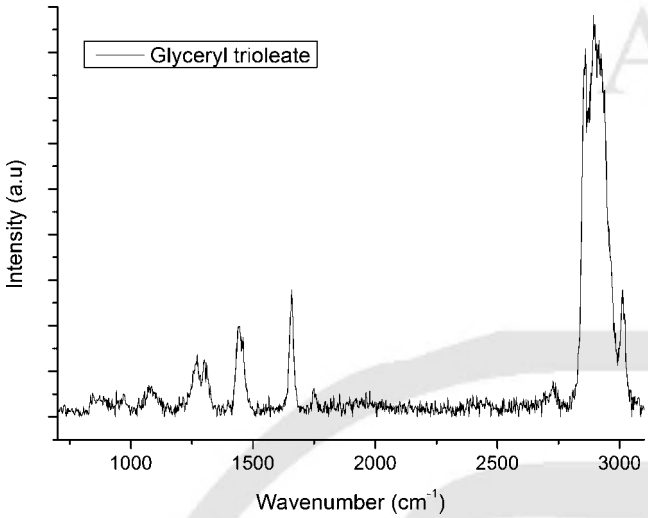

Figure 2. The Raman spectrum of glyceryl trioleate, which is used as a representative to the spectra of generic unsaturated triglyceride.

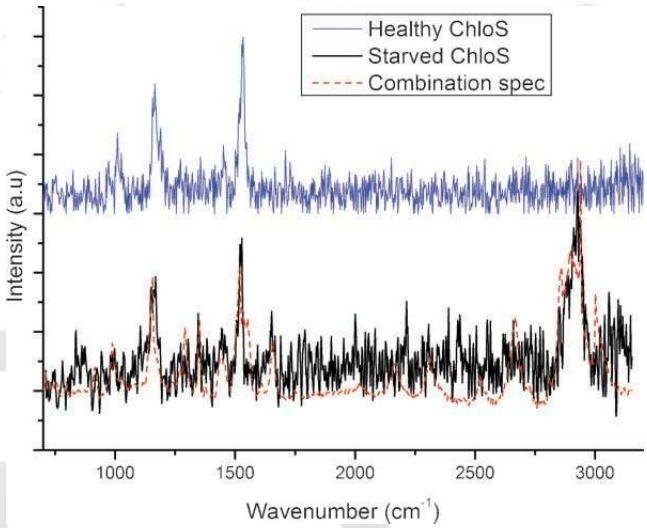

Figure 3. The mean Raman spectrum of starved *C. sorokiniana* (*Starved ChloS*) (black line), and the combined spectrum of contributions from carotenoid, chlorophyll, and triglyceride (dashed red line). The spectrum of healthy *C. sorokiniana* (*Healthy ChloS*) (blue line) is also shown as a comparison.

(Evans et al., 2005; Hellerer et al., 2007; Zhu et al., 2009).

In addition to triglyceride, spectra from pigments should also be considered because they are highly sensitive to the excitation energy and have been reported to contribute significantly to the Raman spectra of many algae (Brahma et al., 1983; Kubo et al., 2000; Heraud et al., 2006, 2007; Wood et al., 2005). Using an excitation wavelength of 488 nm, Chen et al. (2004) showed that most strong and medium peaks of chlorophyll-d coincide with those of chlorophyll-a and b. For various carotenoids, it has been shown that their Raman spectra are close to that of the well-documented β-carotene (Cannizzaro et al., 2003; Parker et al., 1999). β-carotene has intense peaks at ~1,150 cm^{-1} (ν_s(C–C)), ~1,520 cm^{-1} (ν_s(C=C)), and 1,008 cm^{-1} (ρ($C–H_3$), ν(C–C)), and major overtone peaks at 2,320 and 2,667 cm^{-1}. In addition, due to similar chemical structure, we expect the various chlorophyll compounds to produce similar spectra and the various carotenoids to produce similar spectra. Thus, one can use the major Raman peaks specifically associated with chlorophyll-d and those associated with β-carotene to represent generic chlorophylls and carotenoids, respectively. The reference spectra for chlorophyll-d and β-carotene are presented alongside with the experimental algal spectra later in Figure 5.

With the above background information, the Raman spectra of the healthy and starved algae can now be presented in detail. For the spectra of healthy *C. sorokiniana* (*Healthy ChloS*) and *N. oleoabundans* (*Healthy NeoO*) illustrated by Figure 3 (blue line) and Figure 4 (blue line), carotenoid seems to be the only assignable component revealed by the strong peaks at ~1,150 and 1,520 cm^{-1}, and a medium peak at ~1,008 cm^{-1}. This result agrees with the previous investigations by a number of authors (Brahma et al., 1983; Heraud et al., 2006, 2007; Kubo et al., 2000; Wood et al., 2005; Wu et al., 1998), who found carotenoids being the main contributors, and sometimes the sole assignable contributors (Brahma et al., 1983; Kubo et al., 2000), to the Raman spectrum. In theory, algae should be differentiated on a class level by the weaker Raman features in the 920–980 and 1,170–1,230 cm^{-1} regions resulting from the difference in their pigment compositions (Wu et al.,

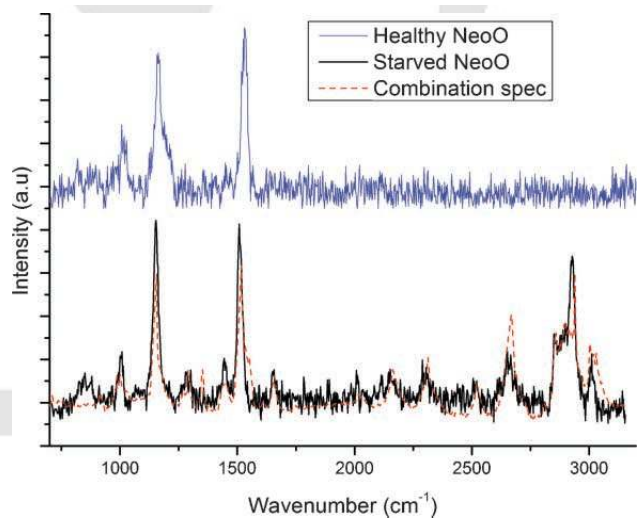

Figure 4. The mean Raman spectrum of starved *N. oleoabundans* (*Starved NeoO*) (black line), and the combined spectrum of contributions from carotenoid, chlorophyll, and triglyceride (dashed red line). The spectrum of healthy *N. oleoabundans* (*Healthy NeoO*) (blue line) is also shown as a comparison.

1998). Such classification would require statistical sampling of a large number of algae, which was not performed in our study.

In contrast to the "simple" Raman spectra illustrated by the healthy algae, the nitrogen-starved samples showed more interesting features. The black lines in Figures 3 and 4 display the average, post-processed Raman spectra of starved *C. sorokiniana* (*Starved ChloS*), and starved *N. oleoabundans* (*Starved NeoO*). Chlorophyll, triglyceride, and carotenoid can be clearly identified by matching the measured Raman spectrum with a combined spectrum of these pure components, shown in red in Figures 3 and 4. For the combination spectra, glyceryl trioleate (representing triglyceride) is the same as that illustrated in Figure 2 previously, while the spectra for β-carotene and chlorophyll-d are from the literature references of Chen et al. (2004) and Parker et al. (1999). To combine these three spectra, optimized normalization factors were used. As shown in Figures 3 and 4, the computed aggregate spectrum and the experimentally obtained mean spectrum agreed well for both starved *C. sorokiniana* and starved *N. oleoabundans*. These two figures also indicate that both of the nitrogen-starved cell types contain high levels of triglycerides compared to their nitrogen-replete counterparts. The single component spectra representing generic carotenoids, chlorophylls, and triglyceride are shown separately in Figure 5.

Chemical Composition Mapping

Figure 6 contains the optical micrographs (100×) of a healthy *N. oleoabundans* agar sample and a starved *N. oleoabundans* cell (*Starved NeoO #2*). Below the optical images are spectral composition maps that were constructed from acquiring spectra according to procedure described in Data Collection and Processing Section. The signal intensity

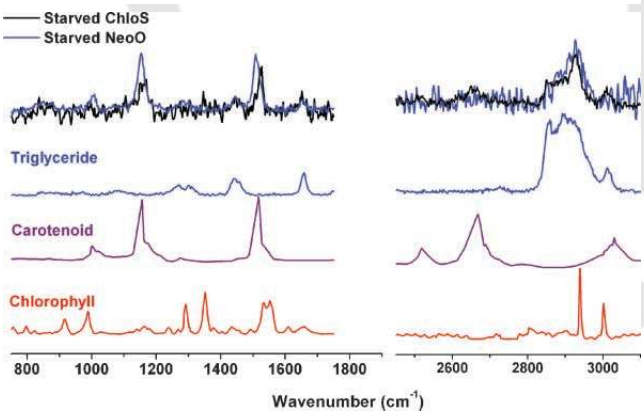

Figure 5. The Raman spectrum of carotenoid (Parker et al., 1999), chlorophyll (Chen et al., 2004), and triglyceride (cf. Fig. 2) and the mean spectra acquired for starved *C. sorokiniana* and starved *N. oleoabundans* in the wavenumber regions of 750–1,750 cm^{-1} and 2,450–3,150 cm^{-1}.

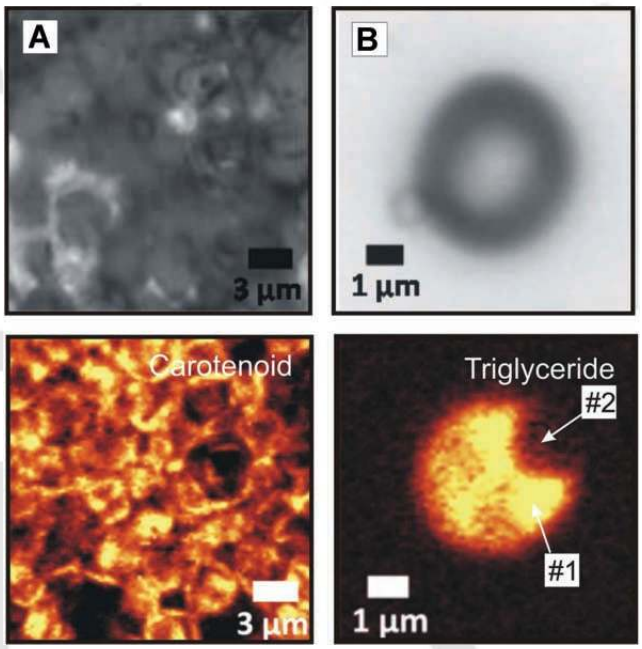

Figure 6. Optical micrographs and background subtracted Raman maps of *N. oleoabundans*: column A shows the image for healthy *N. oleoabundans* in agar (*Healthy NeoO Agar*) and the corresponding chemical mapping for carotenoid; column B displays the optical image of a single starved *N. oleoabundans* cell (*Starved NeoO #2*) and the associated mapping for triglyceride. The high and low lipid regions within the starved cell, of which spectra are analyzed in Figure 7, are marked #1 and #2, respectively.

within the desired wavenumber regions (1,505–1,535 cm^{-1} for carotenoid and 2,800–3,000 cm^{-1} for triglyceride) were measured for every spectra and the map is created such that locations with high intensity are denoted in yellow, medium intensity are denoted in red, and low intensity are denoted in black. The actual resolving power of Raman spectroscopy is limited to be about half of the incident beam wavelength (266 nm, in this case). Then, the diameter of the focal region, which is about 0.5 μm for this study, can limit the resolution. Therefore, the spectra obtained for each location in the chemical composition maps result from the net Raman signal produced by the entire region excited by the incident beam. The locations at which spectra were obtained were separated by 0.2 and 0.1 μm for the carotenoid and lipid maps, respectively. Therefore, adjacent locations (i.e., adjacent pixels) will contain overlapping information. However, each spectrum is unique because it is produced by a unique region excited by the incident beam. The scan region for composition maps shown in column A and column B of Figure 6 are 20 μm × 20 μm and 8 μm × 8 μm, respectively. Every spectrum was acquired with a 0.1 s integration time.

In Figure 6, carotenoid locations are identified for the healthy *N. oleoabundans* agar sample (*Healthy NeoO Agar*) and triglyceride locations are identified for the starved *N. oleoabundans* sample (*Starved NeoO #2*). The optical

image of healthy *N. oleoabundans*, in column (A), shows clumps of algal cells, and the individual cells cannot be distinguished clearly. The carotenoid map indicates distinct locations in which carotenoid is highly concentrated. This result is expected as carotenoid is specifically located within the chloroplast. For starved *N. oleoabundans*, a scan region containing only one isolated cell was selected to perform Raman mapping and triglyceride can be identified clearly. In order to confirm the validity of the lipid composition map, the spectra from two locations (#1 and #2) within the cell are analyzed further in Figure 7. These locations were selected to verify the presence of lipid peaks at location #1 and the absence of lipid peaks at location #2. The major characteristic peaks of triglyceride (cf. Fig. 2) can be identified in the spectrum of region #1, but not in that of region #2. Therefore, the Raman map was successful at identifying the lipid composition in the starved *N. oleoabundans* cell shown. Raman mapping of healthy cells mainly produced noise signals, and are therefore not included for space considerations.

The Raman maps shown in Figure 6 provide a qualitative assessment of the relative composition of algae via Stokes Raman scattering. Growth conditions can have a significant effect on the composition of algal cultures and it is known that *N. oleoabundans* will increase triglyceride production during nitrogen starvation (Tornabene et al., 1983). The Raman map shown in column B of Figure 6 confirms that a significant portion of the cell can be composed of lipids. This study does not determine the sensitivity of Stokes micro-Raman imaging spectroscopy. As mentioned above, there are limitations to the resolution of composition maps which may disallow the detection of components with low abundance. For instance, some amount of triglyceride will be present in healthy and starved cultures of *N. oleoabundans*. In the authors' personal experience, independent studies suggest that healthy and starved cultures of *N. oleoabundans* (grown under similar conditions and for similar duration (i.e., ~15 days) as the cultures in this study) will contain ~2–10% and 15–25% triglyceride by weight, respectively (data not provided. Personal communication, Beal C., University of Texas at Austin, 2009). Applying nitrogen-starvation for a longer duration has been shown to yield even greater lipid content in algae (Hu[Q4] et al., 2007; Tornabene et al., 1983). This indicates that the threshold required for the detection of triglyceride in algal cells by the micro-Raman spectroscopy method presented in this manuscript may be somewhere between the triglyceride content of the healthy and starved cultures used in this study (which were not determined) (cf. Figs. 3 and 4). It is stressed that quantitative composition analysis is beyond the scope of this study. The specific threshold of chlorophyll, carotenoid, or triglyceride content needed to produce reliable Raman signals or the direct correlation between signal intensity and chemical concentration was not determined.

An additional limitation is that fluorescence can overwhelm the component specific peaks in some cases and near infrared excitation wavelengths (e.g., 785 nm) or coherent anti-Stokes Raman spectroscopy may be better suited for algal samples. With additional data processing algorithms and the development of standardized calibrations for the spectral analysis, Raman spectroscopy has the potential to provide a rapid composition analysis tool for the quantification of triglyceride content or other components, such as carotenoids, for the growing industry striving to produce fuels and chemicals from algae.

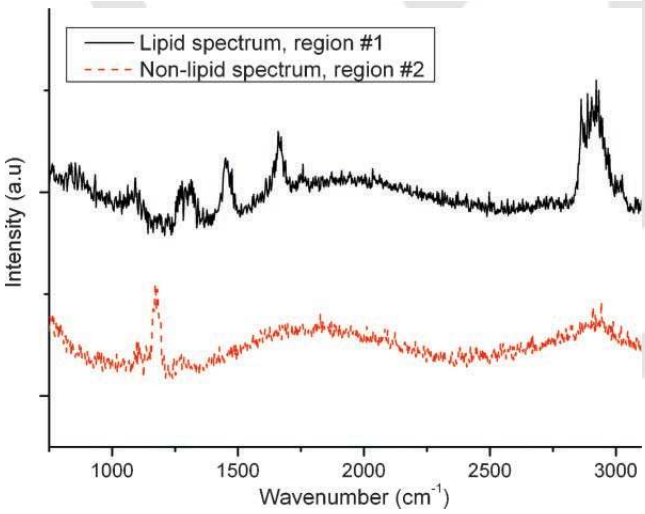

Figure 7. The Raman spectra acquired at positions #1 (yellow region) and #2 (black region) as indicated in Figure 6.

Dynamics of Raman Signal Evolution

Confocal Raman studies on micro-algal cells performed elsewhere (Heraud et al., 2007; Kubo et al., 2000) employed low levels of laser power, that is, below ~1 mW over a spot size of 1–2 μm. This was to avoid photo-damage to the cells and especially to preserve the easily photo-bleached chlorophylls and carotenoids. Nevertheless, the algal spectra obtained mostly contained pronounced sloping fluorescence baselines. In contrast, we employed a much higher power density (~5 mW over a ~0.5 μm spot size) to increase the Stokes Raman scattering response. Under such a constant intense exposure at a single spot in the cell, unexpected spectrum evolution with time was observed. Figure 8 provides an example of a typical series of spectra acquired at consecutive intervals during continuous laser exposure. The relative peak heights, indicative of chemical composition, remain roughly the same over the time of exposure. However, the fluorescence background shows strong time dependence. Contrary to expectation, the consecutive spectra in Figure 8 do not correspond to consecutive times as illustrated by the analysis below.

It is generally accepted that for isolated pigment powders, the fluorescence background level produced during Raman

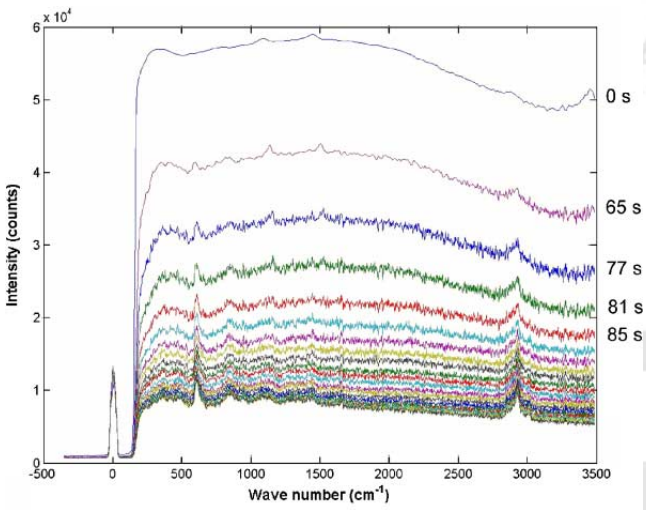

Figure 8. Raman spectrum sampled approximately every 10 s at the center of a fixed starved *N. oleoabundans* cell (*Starved NeoO* Cell 1, cf. Fig. 9, plot b); the laser beam was left on between consecutive data acquisitions.

scattering follows an approximate exponential decay relationship (Splett et al., 1997). In order to examine this relationship, the fluorescence background level is plotted versus the time of exposure. The background level is defined as the sum of all background counts (extracted by RCF) over the 0–3,200 cm^{-1} spectral ranges (cf. Data Collection and Processing Section). A very different phenomenon was found in our samples, illustrated by non-monotonic time dependence of background intensity in Figure 9 for *C. sorokiniana* (*Starved ChloS*) and *N. oleoabundans* (*Starved NeoO*). In all measurements, the first acquisition produced the highest value of fluorescence. This was followed by a large rapid decrease, and then an exponentially slower decrease. Unexpectedly, after some illumination time (which varied for different cells around ~1–2 min), the fluorescence level abruptly returned to a high value and then the decay process repeated itself, sometimes more than once.

Fluctuation in the incident laser power was minimal as demonstrated by the intensity at $\Delta\omega = 0\ cm^{-1}$ which stayed effectively constant (cf. Fig. 8). The fluorescence can be attributed to various carotenoids (Gaier et al., 1991) as well as chlorophylls (Bukin et al., 2008) in the chloroplast. For example, the quenching of chlorophyll fluorescence in LHCII (a major light harvesting antenna protein) was observed to take place on a time scale of milliseconds (Pascal et al., 2005) and so it is not surprising that significant photobleaching of pigments can occur. If the few "abnormal" high intensity events are omitted, the slow decay of fluorescence intensity with time of exposure is apparent. This decay follows a power-law relationship $\sim t^{-x}$ (cf. the insets in Fig. 9), with the exponent $x \sim 0.87$ for *C. sorokiniana* and $x \sim 0.35$ for *N. oleoabundans*. A non-exponential time dependence is usually attributed to collective, cooperative processes and in our case, this may imply a nonlinear absorption effect at higher intensity (Serra and Terentjev, 2008), or be a consequence of complex photosynthetic reactions that occur in chloroplast organelles on absorption of light (Neidhardt et al., 1998). The exact cause for the observed high intensity events is still under investigation. Several possibilities include the movement of a new chloroplast into the beam focus volume (due to random thermal migration or a direct optical trapping effect), as well as another consequence of electronic exchange during the photosynthetic process reset in the chloroplast organelle. Finally, Raman spectroscopy could be conducted with a 785 nm laser which may significantly reduce the background fluorescence. This could be advantageous is some cases, however, the high fluorescence background enabled the documentation of a very interesting phenomenon in this study.

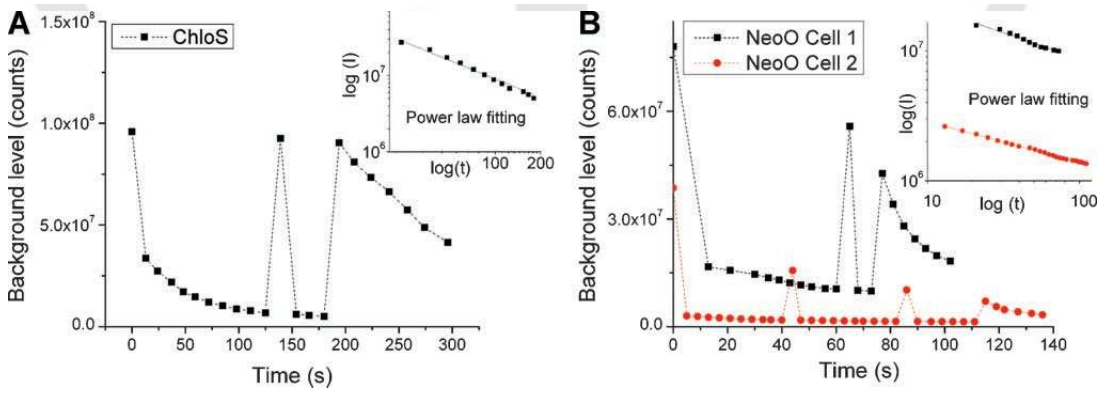

Figure 9. **a**: The background fluorescence intensity level versus the laser exposure time for one starved *C. sorokiniana* cell (*Starved ChloS*). **b**: The fluorescence intensity level versus laser exposure time for two different starved *N. oleoabundans* cells (*Starved NeoO*). The insets demonstrate the power law fitting of the low decay background when the "abnormal" high fluorescence events are omitted.

Conclusion

Two algal species, *C. sorokiniana* (UTEX #1230) and *N. oleoabundans* (UTEX #1185), were tested using conventional Stokes Raman scattering. For both species, only the carotenoid component was able to be assigned in the spectra of healthy cells. On the other hand, the signals from carotenoids, chlorophylls, and triglycerides were clearly identified in the Raman spectra of *C. sorokiniana* and *N. oleoabundans* which had been nitrogen starved. In addition, chemical maps demonstrated that confocal Raman microscopy operating under the Stokes scattering regime is capable of identifying the compound of interest within a single cell down to a few microns. Carotenoids and triglycerides were identified using the filtered Raman mapping technique and the locations of each component within the scanned region could be determined. Unexpected variations in the fluorescence background levels when prolonged laser exposure is applied were observed. The background level followed a generally power-law decaying trend that was interrupted with sudden spikes of high intensity fluorescence events. The general trend of decreasing background level may be explained by the photobleaching of pigments in chloroplasts. However, the high intensity fluorescence events are not yet understood. Overall, this study demonstrates that Stokes Raman spectroscopy is capable of detecting and identifying storage lipids, specifically triglyceride. Conventional Raman scattering thus sees the potential to provide a fast and non-intrusive compositional analysis technique which may enable future in-line or at-line lipid content monitoring. Future experiments should be designed to determine the relationship between the lipid (or triglyceride) concentration in algae and the associated Raman signal intensity in order to establish a standardized lipid quantification method.

References

Begley RF, Harvey AB, Byer RL. 1974. Coherent anti-Stokes Raman spectroscopy. Appl Phys Lett 25:387–390.

Brahma SK, Hargraves PE, Howard WF, Nelson WH. 1983. A resonance Raman method for the rapid detection and identification of algae in water. Appl Spectrosc 37:55–58.

Brandt NN, Brovko OO, Chikishev AY, Paraschuk OD. 2006. Optimization of the rolling-circle filter for Raman background subtraction. Appl Spectrosc 60:288–293.

Bresson S, El Marssi M, Khelifa B. 2005. Raman spectroscopy investigation of various saturated monoacid triglycerides. Chem Phys Lipids 134:119–129.

Bukin OA, Golik SS, Salyuk PA, Baulo EN, Lastovskaya IA. 2008. Efficiency of fluorescence excitation in chlorophyll-a by the second and third harmonics of emission from an ND:YAG laser. J Appl Spectrosc 75:231–235.

Cannizzaro C, Rhiel M, Marison I, von Stockar U. 2003. On-line monitoring of Phaffia rhodozyma fed-batch process with in situ dispersive Raman spectroscopy. Biotechnol Bioeng 83:668–680.

Chao RS, Khanna RK, Lippincott ER. 1975. Theoretical and experimental resonance Raman intensities for the manganate ion. J Raman Spectrosc 3:121–131.

Chen M, Zeng H, Larkuma AWD, Cai ZL. 2004. Raman properties of chlorophyll-d, the major pigment of acaryochloris marina: Studies using both Raman spectroscopy and density functional theory. Spectrochim Acta Part A 60:527–534.

de Gelder J, de Gussem K, Vandenabeele P, Moens L. 2007. Reference database of Raman spectra of biological molecules. J Raman Spectrosc 38:1133–1147.

Demirbas A. 2007. Importance of biodiesel as transportation fuel. Energy Policy 35:4661–4670.

Durret TP, Benning C, Ohlrogge J. 2008. Plant triacylglycerols as feedstocks for the production of biofuels. Plant J 54:593–607.

Evans CL, Potma EO, Puoris'haag M, Cote D, Lin CP, Xie XS. 2005. Chemical imaging of tissue in vivo with video-rate coherent anti-Stoke Raman scattering microscopy. Proc Natl Acad Sci USA 102:16807–16812.

Frank S, Parker ER. 1983a. Applications[Q5] of infrared, Raman, and resonance Raman spectroscopy in biochemistry. Springer. p. 36–39.

Frank S, Parker ER. 1983b. Applications[Q6] of infrared, Raman, and resonance Raman spectroscopy in biochemistry. Springer. p. 10.

Gaier K, Angerhofer A, Wolf HC. 1991. The lowest excited electronic singlet-states of all-trans beta-carotene single-crystals. Chem Phys Lett 187:103–109.

Gillan FT, Johns RB. 1983. Normal-phase HPLC analysis of microbial carotenoids and neutral lipids. J Chromatogr Sci 21:34–38.

Guschina IA, Harwood JL. 2006. Lipids and lipid metabolism in eukaryotic algae. Progr Lipid Res 45:160–186.

Hellerer T, Axang C, Brackmann C, Hillertz P, Pilon M, Enejder A. 2007. Monitoring of lipid storage in Caenorhabditis elegans using coherent anti-Stokes Raman scattering (CARS) microscopy. Proc Natl Acad Sci USA 104:14658–14663.

Hendra PJ, Agbenyega JK. 1993. The Raman Spectra of polymers. New York: John Wiley & Sons. C:1 B p.

Heraud P, Wood BR, Beardall J, McNaughton D. 2006. Effects of pre-processing of Raman spectra on in vivo classification of nutrient status of microalgal cells. J Chem 20:193–197.

Heraud P, Beardall J, McNaughton D, Wood BR. 2007. In vivo prediction of the nutrient status of individual microalgal cells using Raman microspectroscopy. FEMS Microbiol Lett 275:24–30.

Hu Q, Sommerfeld M, Jarvis E, Ghirardi M, Posewitz M, Seibert M, Darzins A. 2008. Microalgal triacylglycerols as feedstocks for biofuel production: Perspectives and advances. Plant J 54:621–639.

Knothe G. 2006. Analyzing biodiesel: Standards and other methods. J Am Oil Chem Soc 83(10):823–833.

Kubo Y, Ikeda T, Yang SY, Tsuboi M. 2000. Orientation of carotenoid molecules in the eyespot of alga: In situ polarized resonance Raman spectroscopy. Appl Spectrosc 54:1114–1119.

Largeau C, Casadevall E, Berkaloff C, Dhamelincourt P. 1980. Sites of accumulation and composition of hydrocarbons in *Botryococcus-braunii*. Phytochemistry (Elsevier) 19:1043–1051.

Li X, Xu H, Wu Q. 2007. Large-scale biodiesel production from microalga *Chlorella protothecoides* through heterotrophic cultivation in bioreactors. Biotechnol Bioeng 98(4):764–771.

Miao X, Wu Q. 2006. Biodiesel production from heterotrophic microalgal oil. Bioresour Technol 97:841–846.

Neidhardt J, Benemann JR, Zhang L, Melis A. 1998. Photosystem-II repair and chloroplast recovery from irradiance stress: Relationship between chronic photoinhibition, light-harvesting chlorophyll antenna size and photosynthetic productivity in Dunaliella salina (green algae). Photosynth Res 56:175–184.

Nischwitz V, Pergantis SA. 2006. Improved arsenic speciation analysis for extracts of commercially available edible marine algae using HPLC-ES-MS/MS. J Agric Food Chem 54:6507–6519.

Oba T, Mimuro M, Wang ZY, Nozawa T, Yoshida S, Watanabe T. 1997. Spectral characteristics and colloidal properties of chlorophyll a' in aqueous methanol. J Phys Chem B 101:3261–3268.

Parker SF, Tavender SM, Dixon NM, Herman HK, Williams KPJ, Maddams WF. 1999. Raman spectrum of beta-carotene using laser lines from green (514.5 nm) to near-infrared (1064 nm): Implications for the characterization of conjugated polyenes. Appl Spectrosc 53:86–91.

Pascal AA, Liu ZF, Broess K, van Oort B, van Amerongen H, Wang C, Horton P, Robert B, Chang WR, Ruban A. 2005. Molecular basis of photoprotection and control of photosynthetic light-harvesting. Nature 436:134–137.

Radmer RJ, Parker BC. 1994. Commercial applications of algae: Opportunities and constraints. J Appl Phycol 6:93–98.

Schmid H, Stich HB. 1995. HPLC-analysis of algal pigments: Comparison of columns, column properties and eluents. J Appl Phycol 7:487–494.

Serra F, Terentjev EM. 2008. Nonlinear dynamics of absorption and photobleaching of dyes. J Chem Phys 128:224510.

Sheehan J, Dunahay T, Benemann R, Roessler G, Weissman C. 1998. A look back at the U.S. department of energy's aquatic species program biodiesel from algae. NREL 580:24190.

Smith E, Dent G. 2005. Modern[Q7] Raman Spectroscopy, A Practical Approach. John Wiley & Sons. p. 24.

Spiro TG, Resonance Raman spectroscopy. 1974. New structure probe for biological chromophores. Acc Chem Res 7:339–344.

Splett A, Splett C, Pilz W. 1997. Dynamics of the Raman background decay. J Raman Spectrosc 28:481–485.

Thompson GA, Jr. 1996. Lipids and membrane function in green algae. Biochim Biophys Acta 1302:17–45.

Tornabene TG, Holzer G, Lien S, Burris N. 1983. Lipid composition of the nitrogen starved green alga Neochloris oleoabundans. Enzyme Microb Technol 5:435–440.

Wood BR, Heraud P, Stojkovic S, Morrison D, Beardall J, McNaughton D. 2005. A portable Raman acoustic levitation spectroscopic system for the identification and environmental monitoring of algal cells. Anal Chem 77:4955–4961.

Wu Q, Nelson WH, Hargraves P, Zhang J, Brown CW, Seelenbinder JA. 1998. Differentiation of algae clones on the basis of resonance Raman spectra excited by visible light. Anal Chem 70:1782–1787.

Xie XS, Yu J, Yang WY. 2006. Living cells as test tubes. Science 312:228–230.

Yang SG, Xia DY, Yang XL, Zhao J. 1991. Effect of algae and water on water color shift. Chinese J Oceanolog Limnolog 9:49–56.

Zhu J, Lee B, Buhman KK, Cheng J. 2009. A dynamic, cytoplasmic triacylglycerol pool in enterocytes revealed by ex vivo and in vivo coherent anti-Stokes Raman scattering imaging. J Lipid Res 50:1080–1089.

Q1: Author: Please check the short title.

Q2: Author: Please add in the reference list.

Q3: Author: Please provide complete location.

Q4: Author: Please add in the reference list.

Q5: Author: Please provide the publisher location.

Q6: Author: Please provide the publisher location.

Q7: Author: Please provide the publisher location.

WILEY
Publishers Since 1807

111 RIVER STREET, HOBOKEN, NJ 07030

*****IMMEDIATE RESPONSE REQUIRED*****

Your article will be published online via Wiley's EarlyView® service (www.interscience.wiley.com) shortly after receipt of corrections. EarlyView® is Wiley's online publication of individual articles in full text HTML and/or pdf format before release of the compiled print issue of the journal. Articles posted online in EarlyView® are peer-reviewed, copyedited, author corrected, and fully citable via the article DOI (for further information, visit www.doi.org). EarlyView® means you benefit from the best of two worlds--fast online availability as well as traditional, issue-based archiving.

Please follow these instructions to avoid delay of publication.

☐ **READ PROOFS CAREFULLY**

- This will be your only chance to review these proofs**. Please note that once your corrected article is posted online, it is considered legally published, and cannot be removed from the Web site for further corrections.**
- Please note that the volume and page numbers shown on the proofs are for position only.

☐ **ANSWER ALL QUERIES ON PROOFS** (Queries for you to answer are attached as the last page of your proof.)

- Mark all corrections directly on the proofs. Note that excessive author alterations may ultimately result in delay of publication and extra costs may be charged to you.

☐ **CHECK FIGURES AND TABLES CAREFULLY**

- Check size, numbering, and orientation of figures.
- All images in the PDF are downsampled (reduced to lower resolution and file size) to facilitate Internet delivery. These images will appear at higher resolution and sharpness in the printed article.
- Review figure legends to ensure that they are complete.
- Check all tables. Review layout, title, and footnotes.

☐ **COMPLETE REPRINT ORDER FORM**

- Fill out the attached reprint order form. It is important to return the form even if you are not ordering reprints. You may, if you wish, pay for the reprints with a credit card. Reprints will be mailed only after your article appears in print. This is the most opportune time to order reprints. If you wait until after your article comes off press, the reprints will be considerably more expensive.

RETURN ☐**PROOFS**
☐**REPRINT ORDER FORM**
☐**CTA (If you have not already signed one)**

RETURN IMMEDIATELY AS YOUR ARTICLE WILL BE POSTED ONLINE SHORTLY AFTER RECEIPT; FAX PROOFS TO 201-748-7670

QUESTIONS? Production Editor
E-mail:bitprod@wiley.com

Refer to journal acronym and article production number
(i.e., BIT 00-001 for Biotechnology and Bioengineering ms 00-001).

WILEY
Publishers Since 1807

COLOR REPRODUCTION IN YOUR ARTICLE

Color figures were included with the final manuscript files that we received for your article. Because of the high cost of color printing, we can only print figures in color if authors cover the expense.

Please indicate if you would like your figures to be printed in color or black and white. Color images will be reproduced online in Wiley *InterScience* at no charge, whether or not you opt for color printing.

You will be invoiced for color charges once the article has been published in print.

Failure to return this form with your article proofs will delay the publication of your article.

JOURNAL **BIOTECHNOLOGY AND BIOENGINEERING**

MS. NO. _____ NO. OF COLOR PAGES _____

TITLE OF MANUSCRIPT _____

AUTHOR(S) _____

No. Color Pages	Color Charges	No. Color Pages	Color Charges	No. Color Pages	Color Charges
1	**500**	**5**	**2500**	**9**	**4500**
2	**1000**	**6**	**3000**	**10**	**5000**
3	**1500**	**7**	**3500**	**11**	**5500**
4	**2000**	**8**	**4000**	**12**	**6000**
Please contact the Production Editor for a quote if you have more than 12 pages of color					

☐ Please print my figures in black and white

☐ Please print my figures in color

☐ Please print the following figures in color:

BILLING ADDRESS: _____

COPYRIGHT TRANSFER AGREEMENT

WILEY-BLACKWELL

Date: _____ Contributor name: _____

Contributor address: _____

Manuscript number (Editorial office only): _____

Re: Manuscript entitled _____

_____ (the "Contribution")

for publication in _____ (the "Journal")

published by _____ ("Wiley-Blackwell").

Dear Contributor(s):
Thank you for submitting your Contribution for publication. In order to expedite the editing and publishing process and enable Wiley-Blackwell to disseminate your Contribution to the fullest extent, we need to have this Copyright Transfer Agreement signed and returned as directed in the Journal's instructions for authors as soon as possible. If the Contribution is not accepted for publication, or if the Contribution is subsequently rejected, this Agreement shall be null and void. **Publication cannot proceed without a signed copy of this Agreement.**

A. COPYRIGHT

1. The Contributor assigns to Wiley-Blackwell, during the full term of copyright and any extensions or renewals, all copyright in and to the Contribution, and all rights therein, including but not limited to the right to publish, republish, transmit, sell, distribute and otherwise use the Contribution in whole or in part in electronic and print editions of the Journal and in derivative works throughout the world, in all languages and in all media of expression now known or later developed, and to license or permit others to do so.

2. Reproduction, posting, transmission or other distribution or use of the final Contribution in whole or in part in any medium by the Contributor as permitted by this Agreement requires a citation to the Journal and an appropriate credit to Wiley-Blackwell as Publisher, and/or the Society if applicable, suitable in form and content as follows: (Title of Article, Author, Journal Title and Volume/Issue, Copyright © [year], copyright owner as specified in the Journal). Links to the final article on Wiley-Blackwell's website are encouraged where appropriate.

B. RETAINED RIGHTS

Notwithstanding the above, the Contributor or, if applicable, the Contributor's Employer, retains all proprietary rights other than copyright, such as patent rights, in any process, procedure or article of manufacture described in the Contribution.

C. PERMITTED USES BY CONTRIBUTOR

1. Submitted Version. Wiley-Blackwell licenses back the following rights to the Contributor in the version of the Contribution as originally submitted for publication:

a. After publication of the final article, the right to self-archive on the Contributor's personal website or in the Contributor's institution's/employer's institutional repository or archive. This right extends to both intranets and the Internet. The Contributor may not update the submission version or replace it with the published Contribution. The version posted must contain a legend as follows: This is the pre-peer reviewed version of the following article: FULL CITE, which has been published in final form at [Link to final article].

b. The right to transmit, print and share copies with colleagues.

2. Accepted Version. Re-use of the accepted and peer-reviewed (but not final) version of the Contribution shall be by separate agreement with Wiley-Blackwell. Wiley-Blackwell has agreements with certain funding agencies governing reuse of this version. The details of those relationships, and other offerings allowing open web use, are set forth at the following website: http://www.wiley.com/go/funderstatement. NIH grantees should check the box at the bottom of this document.

3. Final Published Version. Wiley-Blackwell hereby licenses back to the Contributor the following rights with respect to the final published version of the Contribution:

a. Copies for colleagues. The personal right of the Contributor only to send or transmit individual copies of the final published version in any format to colleagues upon their specific request provided no fee is charged, and further-provided that there is no systematic distribution of the Contribution, e.g. posting on a listserve, website or automated delivery.

b. Re-use in other publications. The right to re-use the final Contribution or parts thereof for any publication authored or edited by the Contributor (excluding journal articles) where such re-used material constitutes less than half of the total material in such publication. In such case, any modifications should be accurately noted.

c. Teaching duties. The right to include the Contribution in teaching or training duties at the Contributor's institution/place of employment including in course packs, e-reserves, presentation at professional conferences, in-house training, or distance learning. The Contribution may not be used in seminars outside of normal teaching obligations (e.g. commercial seminars). Electronic posting of the final published version in connection with teaching/training at the Contributor's institution/place of employment is permitted subject to the implementation of reasonable access control mechanisms, such as user name and password. Posting the final published version on the open Internet is not permitted.

d. Oral presentations. The right to make oral presentations based on the Contribution.

4. Article Abstracts, Figures, Tables, Data Sets, Artwork and Selected Text (up to 250 words).

a. Contributors may re-use unmodified abstracts for any non-commercial purpose. For on-line uses of the abstracts, Wiley-Blackwell encourages but does not require linking back to the final published versions.

b. Contributors may re-use figures, tables, data sets, artwork, and selected text up to 250 words from their Contributions, provided the following conditions are met:

(i) Full and accurate credit must be given to the Contribution.
(ii) Modifications to the figures, tables and data must be noted. Otherwise, no changes may be made.
(iii) The reuse may not be made for direct commercial purposes, or for financial consideration to the Contributor.
(iv) Nothing herein shall permit dual publication in violation of journal ethical practices.

D. CONTRIBUTIONS OWNED BY EMPLOYER

1. If the Contribution was written by the Contributor in the course of the Contributor's employment (as a "work-made-for-hire" in the course of employment), the Contribution is owned by the company/employer which must sign this Agreement (in addition to the Contributor's signature) in the space provided below. In such case, the company/employer hereby assigns to Wiley-Blackwell, during the full term of copyright, all copyright in and to the Contribution for the full term of copyright throughout the world as specified in paragraph A above.

2. In addition to the rights specified as retained in paragraph B above and the rights granted back to the Contributor pursuant to paragraph C above, Wiley-Blackwell hereby grants back, without charge, to such company/employer, its subsidiaries and divisions, the right to make copies of and distribute the final published Contribution internally in print format or electronically on the Company's internal network. Copies so used may not be resold or distributed externally. However the company/employer may include information and text from the Contribution as part of an information package included with software or other products offered for sale or license or included in patent applications. Posting of the final published Contribution by the institution on a public access website may only be done with Wiley-Blackwell's written permission, and payment of any applicable fee(s). Also, upon payment of Wiley-Blackwell's reprint fee, the institution may distribute print copies of the published Contribution externally.

E. GOVERNMENT CONTRACTS

In the case of a Contribution prepared under U.S. Government contract or grant, the U.S. Government may reproduce, without charge, all or portions of the Contribution and may authorize others to do so, for official U.S. Government purposes only, if the U.S. Government contract or grant so requires. (U.S. Government, U.K. Government, and other government employees: see notes at end)

F. COPYRIGHT NOTICE

The Contributor and the company/employer agree that any and all copies of the final published version of the Contribution or any part thereof distributed or posted by them in print or electronic format as permitted herein will include the notice of copyright as stipulated in the Journal and a full citation to the Journal as published by Wiley-Blackwell.

G. CONTRIBUTOR'S REPRESENTATIONS

The Contributor represents that the Contribution is the Contributor's original work, all individuals identified as Contributors actually contributed to the Contribution, and all individuals who contributed are included. If the Contribution was prepared jointly, the Contributor agrees to inform the co-Contributors of the terms of this Agreement and to obtain their signature to this Agreement or their written permission to sign on their behalf. The Contribution is submitted only to this Journal and has not been published before. (If excerpts from copyrighted works owned by third parties are included, the Contributor will obtain written permission from the copyright owners for all uses as set forth in Wiley-Blackwell's permissions form or in the Journal's Instructions for Contributors, and show credit to the sources in the Contribution.) The Contributor also warrants that the Contribution contains no libelous or unlawful statements, does not infringe upon the rights (including without limitation the copyright, patent or trademark rights) or the privacy of others, or contain material or instructions that might cause harm or injury.

CHECK ONE BOX:

☐ Contributor-owned work

ATTACH ADDITIONAL SIGNATURE PAGES AS NECESSARY

Contributor's signature _____ Date _____

Type or print name and title _____

Co-contributor's signature _____ Date _____

Type or print name and title _____

☐ Company/Institution-owned work (made-for-hire in the course of employment)

Company or Institution (Employer-for-Hire) _____ Date _____

Authorized signature of Employer _____ Date _____

☐ U.S. Government work

Note to U.S. Government Employees
A contribution prepared by a U.S. federal government employee as part of the employee's official duties, or which is an official U.S. Government publication, is called a "U.S. Government work," and is in the public domain in the United States. In such case, the employee may cross out Paragraph A.1 but must sign (in the Contributor's signature line) and return this Agreement. If the Contribution was not prepared as part of the employee's duties or is not an official U.S. Government publication, it is not a U.S. Government work.

☐ U.K. Government work (Crown Copyright)

Note to U.K. Government Employees
The rights in a Contribution prepared by an employee of a U.K. government department, agency or other Crown body as part of his/her official duties, or which is an official government publication, belong to the Crown. U.K. government authors should submit a signed declaration form together with this Agreement. The form can be obtained via http://www.opsi.gov.uk/advice/crown-copyright/copyright-guidance/publication-of-articles-written-by-ministers-and-civil-servants.htm

☐ Other Government work

Note to Non-U.S., Non-U.K. Government Employees
If your status as a government employee legally prevents you from signing this Agreement, please contact the editorial office.

☐ NIH Grantees

Note to NIH Grantees
Pursuant to NIH mandate, Wiley-Blackwell will post the accepted version of Contributions authored by NIH grant-holders to PubMed Central upon acceptance. This accepted version will be made publicly available 12 months after publication. For further information, see www.wiley.com/go/nihmandate.

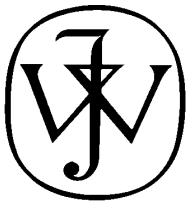

WILEY

Publishers Since 1807

BIOTECHNOLOGY AND BIOENGINEERING

Telephone Number: • Facsimile Number:

To: BIT Production Editor At FAX #: 201-748-7670

From: Dr.

Date:

Re: *Biotechnology* and Bioengineering, ms #

Dear Production Editior

Attached please find corrections to ms# _____. Please contact me should you have any difficulty reading this fax at the numbers listed below.

Office phone:
Email:
Fax:
Lab phone:

I will return color figure proofs (if applicable) once I have checked them for accuracy.

Thank you,

Dr.

E-proofing feedback comments:

C1

WILEY

Publishers Since 1807

REPRINT BILLING DEPARTMENT • 111 RIVER STREET, HOBOKEN, NJ 07030
PHONE: (201) 748-8789; FAX: (201) 748-6326
E-MAIL: reprints@wiley.com

PREPUBLICATION REPRINT ORDER FORM

Please complete this form even if you are not ordering reprints. This form **MUST** be returned with your corrected proofs and original manuscript. Your reprints will be shipped approximately 4 weeks after publication. Reprints ordered after printing will be substantially more expensive.

JOURNAL *Biotechnology and Bioengineering* VOLUME _____ ISSUE _____

TITLE OF MANUSCRIPT _____

MS. NO. _____ NO. OF PAGES _____ AUTHOR(S) _____

No. of Pages	100 Reprints	200 Reprints	300 Reprints	400 Reprints	500 Reprints
	$	$	$	$	$
1-4	**336**	**501**	**694**	**890**	**1052**
5-8	**469**	**703**	**987**	**1251**	**1477**
9-12	**594**	**923**	**1234**	**1565**	**1850**
13-16	**714**	**1156**	**1527**	**1901**	**2273**
17-20	**794**	**1340**	**1775**	**2212**	**2648**
21-24	**911**	**1529**	**2031**	**2536**	**3037**
25-28	**1004**	**1707**	**2267**	**2828**	**3388**
29-32	**1108**	**1894**	**2515**	**3135**	**3755**
33-36	**1219**	**2092**	**2773**	**3456**	**4143**
37-40	**1329**	**2290**	**3033**	**3776**	**4528**

**REPRINTS ARE ONLY AVAILABLE IN LOTS OF 100. IF YOU WISH TO ORDER MORE THAN 500 REPRINTS, PLEASE CONTACT OUR REPRINTS DEPARTMENT AT (201) 748-8789 FOR A PRICE QUOTE.

☐ Please send me _____ reprints of the above article at $ _____

Please add appropriate State and Local Tax for United States orders only. (Tax Exempt No._____) $ _____

Please add 5% Postage and Handling $ _____

TOTAL AMOUNT OF ORDER** $ _____

***International orders must be paid in currency and drawn on a U.S. bank*

Please check one: ☐ Check enclosed ☐ Bill me ☐ Credit Card

If credit card order, charge to: ☐ American Express ☐ Visa ☐ MasterCard

Credit Card No _____ Signature _____ Exp. Date _____

BILL TO:
Name _____
Institution _____
Address _____

SHIP TO: (Please, no P.O. Box numbers)
Name _____
Institution _____
Address _____

Purchase Order No. _____ Phone _____ Fax _____

E-mail _____

Softproofing for advanced Adobe Acrobat Users - NOTES tool

NOTE: ACROBAT READER FROM THE INTERNET DOES NOT CONTAIN THE NOTES TOOL USED IN THIS PROCEDURE.

Acrobat annotation tools can be very useful for indicating changes to the PDF proof of your article. By using Acrobat annotation tools, a full digital pathway can be maintained for your page proofs.

The NOTES annotation tool can be used with either Adobe Acrobat 4.0, 5.0 or 6.0. Other annotation tools are also available in Acrobat 4.0, but this instruction sheet will concentrate on how to use the NOTES tool. Acrobat Reader, the free Internet download software from Adobe, DOES NOT contain the NOTES tool. In order to softproof using the NOTES tool you must have the full software suite Adobe Acrobat 4.0, 5.0 or 6.0 installed on your computer.

Steps for Softproofing using Adobe Acrobat NOTES tool:

1. Open the PDF page proof of your article using either Adobe Acrobat 4.0, 5.0 or 6.0. Proof your article on-screen or print a copy for markup of changes.

2. Go to File/Preferences/Annotations (in Acrobat 4.0) or Document/Add a Comment (in Acrobat 6.0 and enter your name into the “default user” or “author” field. Also, set the font size at 9 or 10 point.

3. When you have decided on the corrections to your article, select the NOTES tool from the Acrobat toolbox and click in the margin next to the text to be changed.

4. Enter your corrections into the NOTES text box window. Be sure to clearly indicate where the correction is to be placed and what text it will effect. If necessary to avoid confusion, you can use your TEXT SELECTION tool to copy the text to be corrected and paste it into the NOTES text box window. At this point, you can type the corrections directly into the NOTES text box window. **DO NOT correct the text by typing directly on the PDF page.**

5. Go through your entire article using the NOTES tool as described in Step 4.

6. When you have completed the corrections to your article, go to File/Export/Annotations (in Acrobat 4.0) or Document/Add a Comment (in Acrobat 6.0).

7. **When closing your article PDF be sure NOT to save changes to original file.**

8. To make changes to a NOTES file you have exported, simply re-open the original PDF proof file, go to File/Import/Notes and import the NOTES file you saved. Make changes and re-export NOTES file keeping the same file name.

9. When complete, attach your NOTES file to a reply e-mail message. Be sure to include your name, the date, and the title of the journal your article will be printed in.